Grafted human-induced pluripotent stem-cell–derived neurospheres promote motor functional recovery after spinal cord injury in mice

Satoshi Nori[a,b,1], Yohei Okada[a,c,1], Akimasa Yasuda[a,b], Osahiko Tsuji[b], Yuichiro Takahashi[a,b], Yoshiomi Kobayashi[a,b], Kanehiro Fujiyoshi[b], Masato Koike[d], Yasuo Uchiyama[d], Eiji Ikeda[e,f], Yoshiaki Toyama[b], Shinya Yamanaka[g], Masaya Nakamura[b,2], and Hideyuki Okano[a,2]

[a]Department of Physiology, [b]Department of Orthopaedic Surgery, [c]Kanrinmaru-Project, School of Medicine, Keio University, Shinjuku, Tokyo 160-8582, Japan; [d]Department of Cell Biology and Neuroscience, Juntendo University Graduate School of Medicine, Bunkyoku, Tokyo 113-8421, Japan; [e]Department of Pathology, School of Medicine, Keio University, Shinjuku, Tokyo 160-8582, Japan; [f]Department of Pathology, Yamaguchi University Graduate School of Medicine, Ube, Yamaguchi 755-8505, Japan; and [g]Center for iPS Cell Research and Application, Kyoto University, Shogoin, Sakyoku, Kyoto 606-8507, Japan

Once their safety is confirmed, human-induced pluripotent stem cells (hiPSCs), which do not entail ethical concerns, may become a preferred cell source for regenerative medicine. Here, we investigated the therapeutic potential of transplanting hiPSC-derived neurospheres (hiPSC-NSs) into nonobese diabetic (NOD)-severe combined immunodeficient (SCID) mice to treat spinal cord injury (SCI). For this, we used a hiPSC clone (201B7), established by transducing four reprogramming factors (Oct3/4, Sox2, Klf4, and c-Myc) into adult human fibroblasts. Grafted hiPSC-NSs survived, migrated, and differentiated into the three major neural lineages (neurons, astrocytes, and oligodendrocytes) within the injured spinal cord. They showed both cell-autonomous and noncell-autonomous (trophic) effects, including synapse formation between hiPSC-NS–derived neurons and host mouse neurons, expression of neurotrophic factors, angiogenesis, axonal regrowth, and increased amounts of myelin in the injured area. These positive effects resulted in significantly better functional recovery compared with vehicle-treated control animals, and the recovery persisted through the end of the observation period, 112 d post-SCI. No tumor formation was observed in the hiPSC-NS–grafted mice. These findings suggest that hiPSCs give rise to neural stem/progenitor cells that support improved function post-SCI and are a promising cell source for its treatment.

stem-cell–based medicine | cell transplantation | neurotrauma | synaptic connection

Stem-cell–based approaches, such as the transplantation of neural stem/progenitor cells (NS/PCs), are promising sources of therapies for various central nervous system disorders (1–3). Previous studies reported functional recovery after transplantation of NS/PCs into the injured spinal cord of rodents and nonhuman primates (4–9). Furthermore, recent studies revealed that embryonic stem cells (ESCs) can generate neural cells including NS/PCs (10–12) and oligodendrocyte precursor cells (OPCs) (13, 14). Therefore, human ESC-based therapies are moving out of the laboratory and into clinical treatments for spinal cord injury (SCI) (12, 13, 15). However, the use of human ESC-based therapies is complicated by ethical concerns in certain countries. To avoid the problems associated with ESCs, we previously established induced pluripotent stem cells (iPSCs) from mouse fibroblasts (16, 17) and confirmed the therapeutic potential of iPSC-derived neurospheres (iPSC-NSs) for treating SCI in animal models (18).

Here, aiming at human iPSC-based therapies for SCI patients, we examined the therapeutic potential of human iPSC-NSs by transplanting them into nonobese diabetic severe combined immunodeficient (NOD-SCID) SCI model mice. We used a clone from human iPSCs (hiPSCs) that we established from adult human dermal fibroblasts by the retroviral transduction of four reprogramming factors; for the clone used in this study, 201B7,

the factors were Oct3/4, Sox2, Klf4, and c-Myc (19). These grafted hiPSC-NSs survived, migrated, and differentiated into the three neural lineages in the injured spinal cord. They promoted angiogenesis and axonal regrowth and preserved myelination, and some formed synapses with host mouse neurons. These positive effects promoted functional recovery that persisted for up to 112 d after SCI, without tumor formation.

These findings indicated that neurospheres derived from hiPSCs are a potential cell source for transplantation therapy for SCI.

Results

Grafted hiPSC-NSs Survived, Migrated, and Differentiated into Three Neural Lineages. Contusive SCI was induced at the Th10 level in NOD-SCID mice, and 5×10^5 Venus$^+$ hiPSC-NSs or PBS was injected into the lesion epicenter, 9 d after injury. To examine the effects of grafted hiPSC-NSs in the injured spinal cord, histological analyses were performed 56 d after SCI [after functional recovery, based on the Basso mouse scale (BMS) score, was observed to plateau]. Ten mice in each group were killed on day 56, and 18 mice grafted with hiPSC-NSs and 16 PBS-injected mice remained. These mice were assessed by BMS and for long-term safety of the grafted hiPSC-NSs, 112 d after SCI (Table S1).

On day 56, the grafted hiPSC-NSs had survived and migrated into the host spinal cord (Fig. 1 A and B). To examine their differentiation potentials, we performed immunohistochemical analyses and quantified the proportion of Venus$^+$ cells immunopositive for cell-type–specific markers. The engrafted hiPSC-NSs differentiated into neuronal nuclei (NeuN)$^+$ and β-tubulin isotype III (βIII tubulin)$^+$ neurons, glial fibrillary acidic protein (GFAP)$^+$ astrocytes, and adenomatous polyposis coli CC-1 (APC)$^+$ oligodendrocytes (Fig. 1 C–F). The βIII tubulin$^+$/Venus$^+$ neurons comprised $49.1 \pm 2.0\%$ of the Venus$^+$ cells, and the mature NeuN$^+$/Venus$^+$ neurons comprised $22.9 \pm 1.0\%$. Thus, 56 d after SCI, about 50% of the grafted hiPSC-NSs had differentiated into neurons, about half of which were mature neurons. GFAP$^+$/Venus$^+$ astrocytes comprised $17.0 \pm 1.2\%$, but APC$^+$/Venus$^+$ oligodendrocytes were rare ($3.0 \pm 0.4\%$). Nestin$^+$/Venus$^+$ NS/PCs made up $10.7 \pm 2.2\%$ of the total (Fig. 1G).
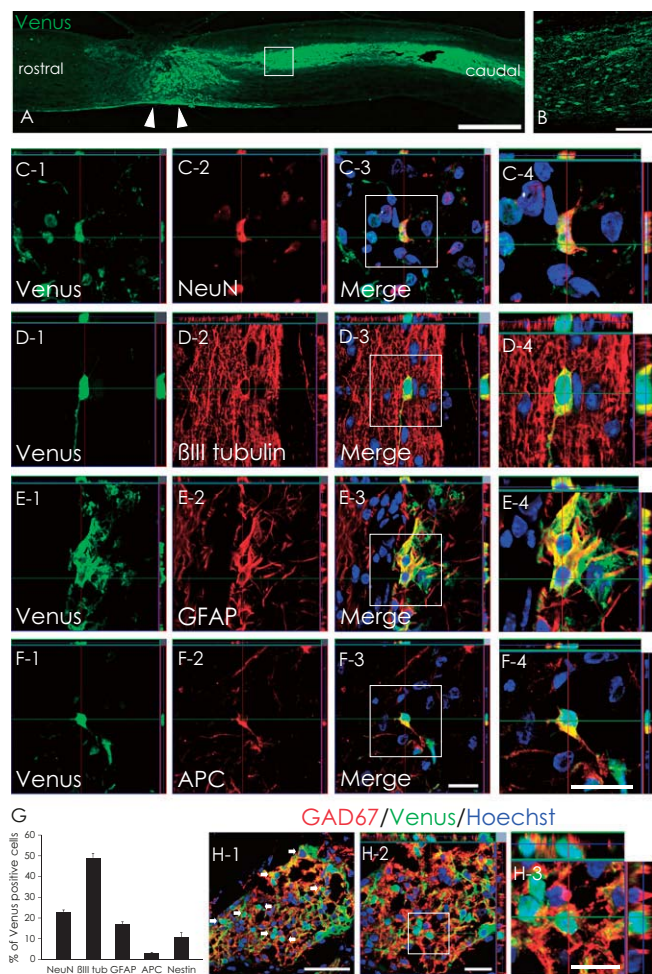
NEUROSCIENCE

Fig. 1. In vivo differentiation of hiPSC-NSs. (*A* and *B*) Venus⁺ hiPSC-NSs were integrated at or near the lesion epicenter (arrowheads). (Scale bars, 1000 μm in *A*; 100 μm in *B*.) (*C–F*) Representative images of Venus⁺-grafted cells labeled with the neural markers NeuN⁺ (mature neurons) (*C*); βIII tubulin⁺ (all neurons) (*D*); GFAP⁺ astrocytes (*E*); and APC⁺ oligodendrocytes (*F*). (Scale bar, 20 μm.) (*G*) Percentages of cell-type–specific marker-positive cells among the Venus⁺-grafted cells 56 d after SCI. Values are means ± SEM (*n* = 4). (*H*) Most hiPSC-derived neurons differentiated into GAD67⁺ (GABAergic) neurons. (Scale bars, 50 μm in *H-1*; 20 μm in *H-2*; and 10 μm in *H-3*.)

Because 22.9% of the hiPSC-NSs differentiated into mature neurons, we next examined their neurotransmitter phenotype, using neurotransmitter-specific markers. Of the Venus⁺ cells, 15.8 ± 2% were glutamic acid decarboxylase 67 (GAD67)⁺, indicating that 69% (15.8/22.9% = 69.0%) of the hiPSC-NS–derived mature neurons were GABAergic (Fig. 1*H*). We also found small numbers of Venus⁺ tyrosine hydroxylase (TH)⁺ neurons and choline acetyltransferase (ChAT)⁺ cholinergic neurons (Fig. S1 *A* and *B*).

Synapse Formation Between hiPSC-Derived Neurons and Host Mouse Neurons. To evaluate the ability of the hiPSC-NS–derived neurons to integrate with the host neural circuitry, triple immunostaining was performed with antibodies to human nuclear protein (HNu), βIII tubulin, and the presynaptic protein Bassoon (Bsn). The anti-Bsn antibody is a monoclonal that selectively recognizes mouse and rat, but not human epitopes. Grafted βIII tubulin⁺/HNu⁺ cells in the neural parenchyma were observed in contact with the synaptic boutons of host neurons (Fig. 2*A*). In addition, triple immunostaining for HNu, βIII tubulin, and human-specific synaptophysin (hSyn) revealed dense fields of
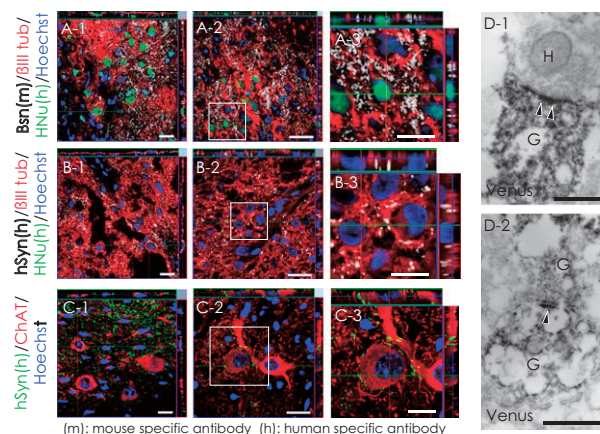

Fig. 2. Evidence for synapse formation between hiPSC-derived neurons and host mouse spinal cord neurons. (*A*) Sections were triple-stained with HNu (green), βIII tubulin (red), and the presynaptic marker Bassoon (Bsn, white). The Bsn antibody used here recognized the rat and mouse, but not human, protein. (*B*) Sections triple-stained for HNu (green), βIII tubulin (red), and the human-specific presynaptic marker hSyn (white). (*C*) Confocal images showing a large number of somatic and dendritic terminals from graft-derived nerve cells on host motor neurons at the ventral horns. (*D*) Electron microscopy showing synapse formation between host mouse neurons and graft-derived Venus⁺ (black) human neurons: the pre- and postsynaptic structures indicated transmission from a host neuron to a graft-derived neuron (*D-1*) and from a graft-derived neuron to a graft-derived neuron (*D-2*). H, host neuron; G, graft-derived neuron; arrowheads, postsynaptic density. (Scale bars, 20 μm in *A-1*, *A-2*, *B-1*, *B-2*, *C-1*, and *C-2*; 10 μm in *A-3*, *B-3*, and *C-3*; and 0.5 μm in *D*.)

boutons apposed to βIII tubulin⁺/HNu⁻ host mouse neurons (Fig. 2*B*). These host neurons in the ventral gray matter were ChAT⁺, and some of the boutons represented graft-specific terminals (Fig. 2*C*). Immunoelectron microscopy revealed Venus⁺ (i.e., human) presynaptic and postsynaptic structures and synapses between host mouse neurons and Venus⁺ hiPSC-derived neurons at the injured site (Fig. 2*D*).

Transplantation of hiPSC-NSs Enhanced Angiogenesis and Axonal Regrowth but Did Not Induce Abnormal Innervation of Pain-Related CGRP⁺ Afferents After SCI. To evaluate the effects of hiPSC-NS transplantation on angiogenesis after SCI, immunohistochemical analyses for platelet endothelial cell adhesion molecule-1 (PECAM-1) were performed. There were significantly more PECAM-1⁺ blood vessels at the lesion epicenter in the hiPSC-NS group than in the control group (Fig. 3 *A–C*). To determine the source of the angiogenic signals, we examined the vascular endothelial growth factor (VEGF) expression in the grafted spinal cord by immunohistochemistry (Fig. 3*D*). Quantitative analyses revealed that the VEGF⁺ area at the lesion epicenter was significantly larger in the hiPSC-NS group than in the control group (Fig. 3*E*). Furthermore, both GFAP⁺/Venus⁺ hiPSC-derived astrocytes (Fig. 3*F*) and GFAP⁺/Venus⁻ host mouse astrocytes expressed VEGF (Fig. 3*G*), consistent with the results of RT-PCR (Fig. 3 *H* and *I*). Note that the mouse *Vegf* mRNA expression level was higher in the hiPSC-NS–grafted mice than in PBS-injected mice.

Because angiogenesis generally improves tissue sparing, we examined the atrophic changes of the injured spinal cord by hematoxylin–eosin (H&E) staining. Unlike the hiPSC-NS group, atrophic changes of the injured spinal cord were prominent in the control group (Fig. 3 *J* and *K*). Quantitative analysis revealed significant differences in the transverse area of the spinal cord between the control and hiPSC-NS group, suggesting that the hiPSC-NS transplantation prevented atrophy of the injured spinal cord (Fig. 3*L*). Luxol fast blue (LFB) staining also revealed
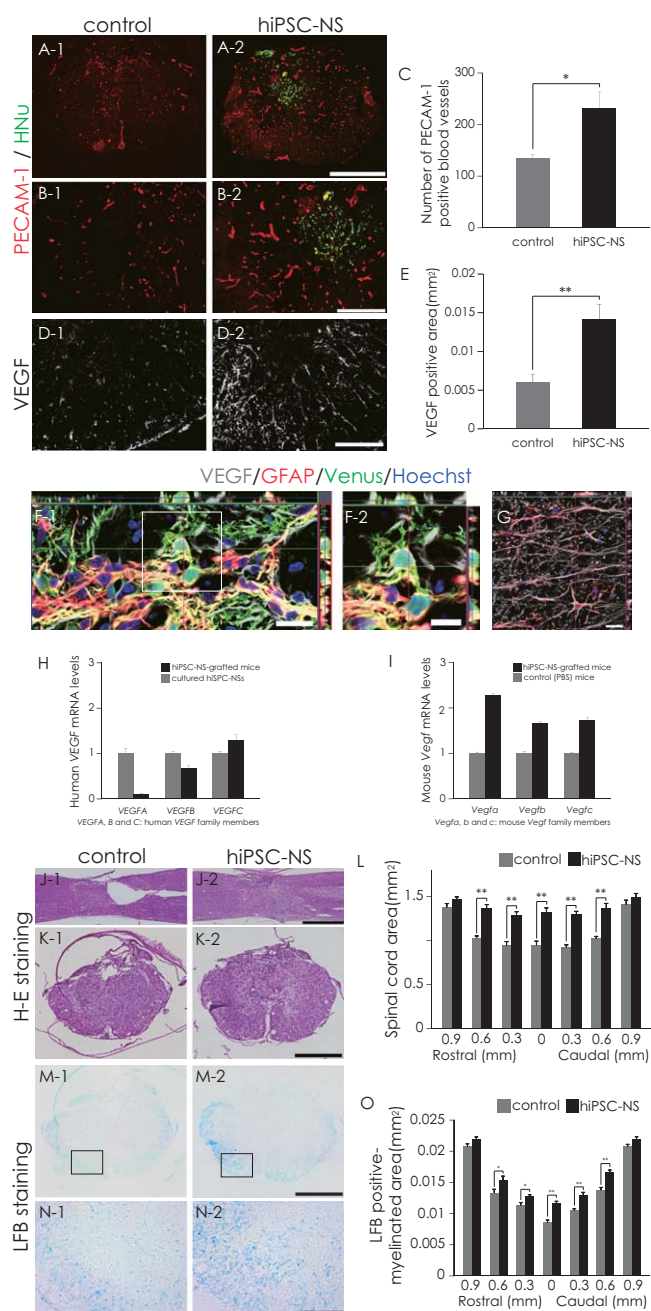
Fig. 3. Transplanted hiPSC-NSs enhanced angiogenesis and prevented atrophic changes and demyelination after SCI. (*A* and *B*) Representative images of PECAM-1$^+$ blood vessels. (*C*) Quantitative analysis of PECAM-1$^+$ blood vessels at the lesion epicenter. Values are means ± SEM (*n* = 4). (*D*) Representative images of axial sections stained for VEGF. (*E*) Quantitative analysis of the VEGF$^+$ area at the lesion epicenter. Values are means ± SEM (*n* = 4). (*F* and *G*) Expression of VEGF in GFAP$^+$ astrocytes among Venus$^+$-graft–derived human cells (yellow indicates VEGF$^+$, GFAP$^+$, and Venus$^+$ cells) (*F*) and host mouse-derived cells (*G*) in the spinal cord. (*H*) Expression of human *VEGF* mRNA (*VEGFA*, -*B*, and -*C* are the human *VEGF* family members) 5 d after the hiPSC-NSs were transplanted (black bars) compared with cultured hiPSC-NSs before transplantation (gray bars). Values are means ± SEM (*n* = 3, each). Human *VEGF* expression was undetectable in the spinal cord of mice treated with PBS. (*I*) Expression of mouse *Vegf* mRNA (*Vegfa*, -*b*, and -*c* are the mouse *Vegf* family members) 5 d after hiPSC-NS transplantation (black bars) or PBS injection (gray bars) into the spinal cord. The mouse *Vegf* expression level was higher in the hiPSC-NS–grafted mice than in PBS-injected mice. Values are means ± SEM (*n* = 3, each). (*J* and *K*) Representative H&E-stained images of sagittal and axial sections at the lesion epicenter 56 d after SCI. (*L*) Quantitative analysis of the spinal cord area measured in H&E-

stained axial sections at different regions. Values are means ± SEM (*n* = 6). (*M* and *N*) Representative LFB-stained images of the axial sections at the lesion epicenter 56 d after SCI. (*O*) Quantitative analysis of the myelinated area by LFB-stained axial sections at different regions. Values are means ± SEM (*n* = 6). *$P < 0.05$, **$P < 0.01$. (Scale bars, 500 µm in *A*, *K*, and *M*; 200 µm in *B*; 100 µm in *D* and *N*; 20 µm in *F-1* and *G*; 10 µm in *F-2*; and 1,000 µm in *J*.)

a greater preservation of myelinated areas in the hiPSC-NS group compared with the control group (Fig. 3 *M–O*).

To evaluate the effects of hiPSC-NS transplantation on axonal regrowth after SCI, we examined the expression of neurofilament 200 kDa (NF-H), 5-hydroxytrytamine (5HT), and growth-associated protein 43 (GAP43) in the injured spinal cord by immunohistochemistry. There were significantly more NF-H$^+$ neuronal fibers in the hiPSC-NS group than in the control group (Fig. 4 *A* and *B*). 5HT$^+$ fibers, descending serotonergic raphespinal tract axons that are important for the motor functional recovery of hind limbs (20–22), were observed at the lumbar intumescence in all mice (Fig. 4*C*). Contusive SCI resulted in a significant decrease in the number of 5HT$^+$ fibers. Relative to mice at 7 d after SCI (2 d before the transplantation), by 56 d after SCI a slight but significant increase in the 5HT$^+$ fiber area was seen in the control group, and the hiPSC-NS group showed an even greater enhancement (Fig. 4 *C* and *D*).

GAP43$^+$ axons, which are regrowing (23), were detected in the distal cords of all mice, but in the hiPSC-NS group, there were significantly more GAP43$^+$ fibers in the ventral region 1 mm caudal to the lesion epicenter (Fig. 4 *E* and *F*), suggesting that the hiPSC-NS transplantation promoted axonal regrowth in the injured spinal cord. We also observed hiPSC-NS–derived astrocytes closely associated with NF-H$^+$ fibers and 5HT$^+$ fibers (Fig. 4 *G* and *H*). Moreover, RT-PCR revealed the expression of neurotrophic factors (NGF, BDNF, and hepatocyte growth factor, HGF), which are associated with the axonal growth and survival of existing neurons, by both the grafted human cells and the host mouse tissues (Fig. 4 *I* and *J*).

To examine the effect of hiPSC-NSs on structural changes in pain afferents entering the dorsal horn of the spinal cord above and below the injured spinal segments, we investigated the distribution of calcitonin gene-related peptide (CGRP$^+$) fibers, which are involved in peripheral and spinal pain mechanisms (6, 24, 25). We quantified the areas of CGRP$^+$ fibers in lamina III, 4 mm rostral and 4 mm caudal to the lesion epicenter. There were no significant differences in the areas of CGRP$^+$ fibers in lamina III between the hiPSC-NS and control groups (Fig. S2 *A–C*).

Transplanted hiPSC-NSs Promoted Motor Functional and Electrophysiological Recovery After SCI. We evaluated the motor functional recovery by BMS score, Rotarod test, and the DigiGait system. The BMS score showed significantly better functional recovery in the hiPSC-NS than the control group 21 d after SCI and thereafter (Fig. 5*A*). In the Rotarod test, the hiPSC-NS group showed a significantly longer running time than the control group 56 d post-SCI (Fig. 5*B*). The DigiGait system measures the treadmill gait, as an objective evaluation of motor function (26, 27). Whereas all of the hiPSC-NS–grafted mice (*n* = 18) could walk on the treadmill at 8 cm/s, a subset of the control mice (4 out of 16) could not maintain this speed. The profile of stride length at 8 cm/s clearly demonstrated a significantly better recovery of motor function in the hiPSC-NS–grafted mice compared with the 12 control mice that could walk at this speed (Fig. 5*C*).

Motor-evoked potential (MEP) was used to measure the functional recovery in all of the mice electrophysiologically. The latency of the motor-evoked potential was also measured, from the onset of stimulus to the first response of each wave. At 112 d after SCI, waves were detected in most of the hiPSC-NS group (14 of 17 mice), but none were detected in the control group (0 of 15 mice) (Fig. 5*D*). The average signal-to-response latency in the hiPSC-NS group was 4.6 ± 0.1 ms. Consistent with the
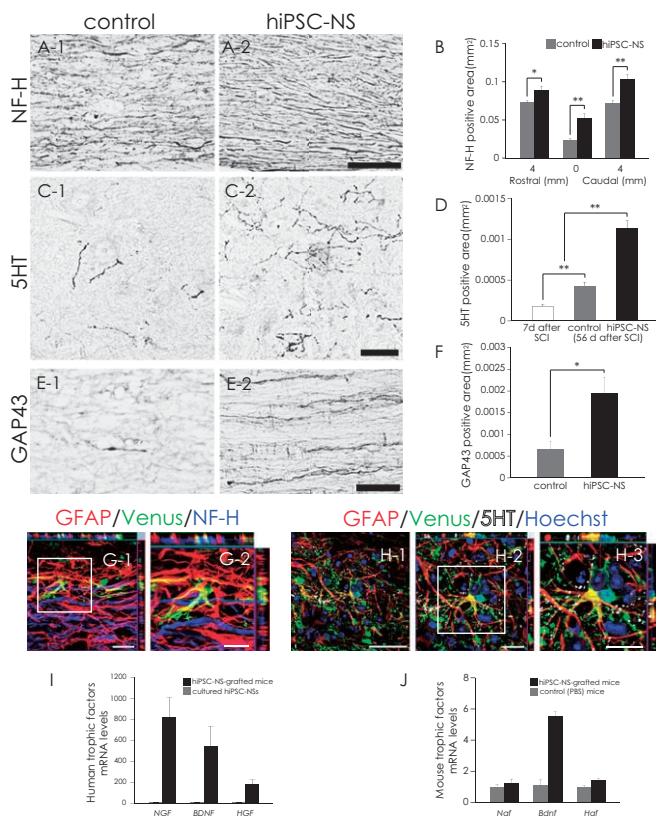
NEUROSCIENCE

Fig. 4. Transplanted hiPSC-NSs enhanced axonal growth after SCI. (*A*) Representative images of sagittal sections stained for NF-H at the lesion epicenter. (*B*) Quantitative analysis of the NF-H$^+$ area. Values are means ± SEM (n = 4). (*C*) Representative images of axial sections stained for 5HT at the lumbar intumescence. (*D*) Quantitative analysis of the 5HT$^+$ area at the lumbar intumescence in axial sections. Values are means ± SEM (n = 6 each in the 7 d and control 56 d after SCI groups, and n = 5 in the hiPSC-NS (56 d after SCI) group). (*E*) Representative images of midsagittal sections stained for GAP43 in the ventral region 1 mm caudal to the lesion epicenter. (*F*) Quantitative analysis of the GAP43$^+$ area in midsagittal sections. Values are means ± SEM (n = 4). (*G* and *H*) NF-H$^+$ neural fibers and 5HT$^+$ (serotonergic) fibers extended in association with GFAP$^+$/Venus$^+$-graft–derived human astrocytes. (*I*) Expression of human neurotrophic factor mRNAs (*NGF*, *BDNF*, and *HGF*) 5 d after hiPSC-NS transplantation (black bars) compared with cultured hiPSC-NSs before transplantation (gray bars). Values are means ± SEM (n = 3, each). (*J*) Expression of mouse neurotrophic factor mRNAs (*Ngf*, *Bdnf*, and *Hgf*) 5 d after hiPSC-NS transplantation (black bars) or PBS injection (gray bars) into the spinal cord. Values are means ± SEM (n = 3, each). *P < 0.05, **P < 0.01. (Scale bars, 100 μm in *A*; 50 μm in *C*, *E*, and *H-1*; 20 μm in *G-1*, *H-2*, and *H-3*; and 10 μm in *G-2*.)

electrophysiology results, α-CaM kinase 2$^+$ descending motor axons were observed to persist in the lesion epicenter in the hiPSC-NS group (Fig. S3).

Long-Term Observation Revealed No Tumor Formation After hiPSC-NS Transplantation. To investigate the long-term safety of the grafted hiPSC-NSs, we extended the follow-up period to 112 d after SCI. Motor functional recovery was maintained in the hiPSC-NS group for the entire period (Fig. 6*A*), the hiPSC-NS–grafted mice showed no tumor formation (Fig. 6*B*), and the grafted cells exhibited normal neural differentiation (Fig. 6*C*). We determined the proportion of Venus$^+$ grafted cells that were immunopositive for each cell-type–specific marker 112 d after SCI. The grafted hiPSC-NSs had differentiated into NeuN$^+$ (40.2 ± 2.8%), βIII tubulin$^+$ (50.7 ± 2.0%), GFAP$^+$ (18.1 ± 2.2%), APC$^+$ (8.9 ± 1.6%), and Nestin$^+$ (7.5 ± 1.0%) cells. For comparison, at 56 d after SCI, the grafted cells had differentiated
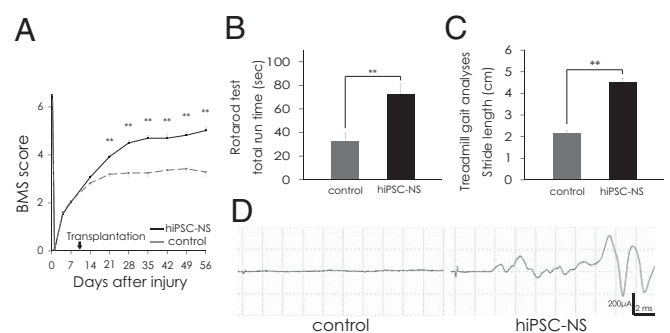

Fig. 5. Transplanted hiPSC-NSs promoted motor functional and electrophysiological recovery after SCI. (*A*) Motor function in the hindlimbs was assessed weekly by the BMS score for 56 d. Values are means ± SEM. (*B*) Rotarod test 56 d after SCI. Graph shows the total run time. Values are means ± SEM. (*C*) Treadmill gait analysis using the DigiGait system 56 d after SCI. Graph shows stride length. Values are means ± SEM. (*D*) Electrophysiological analysis performed 112 d after SCI. MEP waves were detected in most of the hiPSC-NS group (14 out of 17), whereas they were not detected in the control group (0 out of 15). **P < 0.01. Behavioral analyses were assessed by two observers who were blind to the treatment.

into NeuN$^+$ (22.9 ± 1.0%), βIII tubulin$^+$ (49.1 ± 2.0%), GFAP$^+$ (17.0 ± 1.2%), APC$^+$ (3.0 ± 0.4%), and Nestin$^+$ (10.7 ± 2.2%) cells (Fig. 6*D*). Notably, significantly higher percentages of NeuN$^+$ mature neurons and APC$^+$ oligodendrocytes were present at 112 d than at 56 d after SCI, whereas the percentage of graft-derived human Nestin$^+$ NS/PCs slightly decreased. We also examined the amount of proliferation among the grafted cells by K_i-67 labeling. The percentage of K_i-67$^+$/HNu$^+$ cells was significantly decreased between 56 d post-SCI (1.1 ± 0.2%) and 112 d post-SCI (0.7 ± 0.1%). The K_i-67$^+$/HNu$^+$ cells were dispersed throughout the graft area without evidence of clustering at particular sites.

Discussion

In the present study, we used clone 201B7 of hiPSC-derived neurospheres as a cell source to treat SCI in adult NOD-SCID mice. We demonstrated that the hiPSC-NSs differentiated into neurons, astrocytes, and oligodendrocytes in the injured spinal cord and promoted motor functional recovery. Hypothetically, the transplantation of hiPSC-NSs could result in a wide range of positive effects, including angiogenesis, axonal regeneration, and local-circuitry reconstruction, which have been reported in previous studies using rodent ESCs or iPSCs for SCI treatment (12, 18). All these mechanisms could contribute to motor functional recovery after hiPSC-NS transplantation for SCI.

Angiogenesis after SCI promotes endogenous repair and supports axonal outgrowth (28, 29). Here we observed that the transplantation of hiPSC-NSs enhanced angiogenesis and tissue sparing after SCI. Astrocytes express angiogenic growth factors such as VEGF under hypoxic conditions (12, 30, 31), and we observed that the hiPSC-derived astrocytes and host astrocytes expressed VEGF, suggesting that the transplantation of hiPSC-NSs promoted VEGF expression in both host- and graft-derived astrocytes.

Motor functional recovery was also supported by the axonal regrowth that was promoted by the transplanted hiPSC-NSs. Our immunohistochemical analyses revealed grafted hiPSC-derived GFAP$^+$ astrocytes closely associated with NF-H$^+$ and 5HT$^+$ fibers. Graft-derived astrocytes are reported to promote the regrowth of NF-H$^+$ and 5HT$^+$ fibers by offering a growth-permissive substrate (12, 18, 32). Furthermore, neurotrophic factors such as NGF, BDNF, and HGF play critical roles in axonal growth and in the survival of existing neurons (33–38). Consistent with these reports, we observed that hiPSC-NS transplantation promoted axonal regrowth at the distal spinal cord. Because our treatment induced axonal regrowth, we also exam-
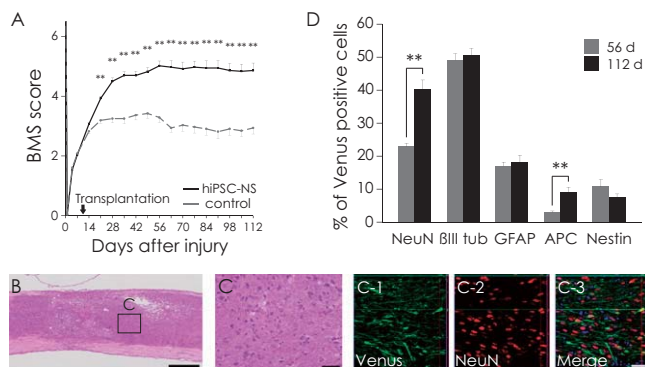
Fig. 6. Long-term observation revealed no tumor formation after hiPSC-NS transplantation. (*A*) For 112 d, motor function in the hindlimbs was assessed weekly by the BMS score. Values are means ± SEM. (*B*) Representative H&E image of hiPSC-NS–grafted mice. (*C*) Boxed area in *B*. (*C-1–C-3*) Immunohistochemistry showing normal neural differentiation of the grafted cells. (*D*) Percentages of cell-type–specific marker-positive cells among the Venus⁺ human cells 56 and 112 d after SCI. Values are means ± SEM (*n* = 4 and 5, respectively). **P < 0.01. (Scale bars, 500 μm in *B*; and 50 μm in *C*.)

ined the pain afferents entering lamina III of the spinal cord, which is closely associated with NS/PC-transplantation–induced allodynia (6). Our analysis revealed no significant differences between the hiPSC-NS and control groups. Thus, although allodynia was not assessed, our morphological data suggested that hiPSC-NS transplantation did not induce abnormal innervation by pain afferents, in contrast to a previous study in which NS/PCs derived from adult rat spinal cord were transplanted into a rat SCI model (6).

The motor functional recovery observed in this study may also be due to the formation of synapses between hiPSC-derived neurons and host mouse spinal cord neurons. Our present data support the potential for grafted hiPSC-NSs to form synapses with host neurons in the injured spinal cord. Previous studies have shown post-SCI functional improvements associated with intraspinal grafts containing neuronal progenitors either alone or in combination with other cells or interventions (4, 7, 39–43). Such studies also report that graft-derived human neurons can receive projections from host mouse neurons and that their extended processes make synapses with host neurons (39). It is likely that local neurons in the lesioned area (a mixture of preserved host neurons and graft-derived neurons) transmit signals by relay.

We observed that most of the hiPSC-derived mature neurons were GABAergic, a neurotransmitter type that plays important roles in the spinal cord by controlling the levels of motoneuronal output and sensory input, by modulating primary afferent transmitter release, and by direct postsynaptic inhibition of motoneurons (44, 45). Furthermore, hypofunctioning spinal GABAergic inhibition is involved in pathological pain states that develop due to SCI (46). Thus, synapse formation by donor-derived GABAergic neurons might be important for motor coordination within the spinal neuronal network and for the suppression of SCI-induced spasticity (8, 47) and pain (46).

The greatest potential drawback of hiPSC-based therapies is their potential for tumorigenicity. Therefore, we observed the treated animals for an extended period. Not only was functional recovery maintained in the hiPSC-NS group for 112 d after SCI, but no tumor formation occurred at all. Quantitative analysis of the phenotype of the grafted hiPSC-NSs revealed an increase in the percentages of NeuN⁺ mature neurons and APC⁺ oligodendrocytes at 112 d compared with 56 d after SCI, showing that most of the grafted hiPSC-NSs successfully differentiated into mature neural cells over time. Some Nestin⁺/HNu⁺ cells and K_i-67⁺/HNu⁺ cells were still present at 112 d post-SCI, although their proportions were lower than at 56 d after SCI, indicating

that some grafted cells remained as NS/PCs. However, no evidence of excessive proliferation, clusters of proliferating cells, or other signs of tumor formation were observed in any of the transplant-receiving mice. Collectively, the lack of tumors, increase in NeuN numbers over time, and low Nestin and K_i-67 numbers support the possibility that this approach will be safe in humans.

Consistent with our findings, previous studies using human fetal NS/PCs showed some Nestin⁺/HNu⁺ cells that were negative for the proliferative markers K_i-67 and proliferating cell nuclear antigen in the striatum of NOD-SCID mice, 6 mo after transplantation (48), 28–34% Nestin⁺/HNu⁺, and 2–4% K_i-67⁺/HNu⁺ cells were in the spinal cord of NOD-SCID mice 4 mo after transplantation (5), and 11–14% Nestin⁺/HNu⁺ and 3–5% K_i-67⁺/HNu⁺ cells were in the spinal cord of nude rats 6 mo after transplantation (49). Notably, no tumor formation was observed in any of these studies, despite the presence of Nestin⁺- and K_i-67⁺–grafted cells, even after long-term observation.

Recently, clinical trials of human stem-cell–based therapy for SCI have been launched, using human NS/PCs (4, 5) or human ESC-derived OPCs (15). In this paradigm, OPC-mediated restoration of myelination and trophic effects are the most likely mechanisms for the resulting benefits. Besides overcoming concerns about immune responses and the ethics of using human ESCs (hESCs), our present study suggests that grafted hiPSC-NSs might be more beneficial than hESCs, because the hiPSC-NSs gave rise to GABAergic neurons, which can help to suppress SCI-induced spasticity and pain (8, 46, 47). In addition, we found that hiPSC-NSs differentiated into astrocytes and oligodendrocytes, which can exert positive effects through both cell-autonomous and noncell-autonomous (trophic) mechanisms. Nevertheless, our present results are only a first step toward clinical applications. In our future studies, the safety and effectiveness of hiPSC-derived NS/PCs will be more intensively investigated, for example, using nonhuman primate SCI models (8). In particular, hiPSCs established by delivering the reprogramming factors using a different method, such as an integration-free virus system (50), or a virus-free (51) or transgene-free system (52–54), or by using (HLA)-homozygous donor-derived cells (55), should be evaluated.

Materials and Methods

NEUROSCIENCE

1. Björklund A, Lindvall O (2000) Cell replacement therapies for central nervous system disorders. Nat Neurosci 3:537–544.
2. Gage FH (2000) Mammalian neural stem cells. Science 287:1433–1438.
3. Lindvall O, Kokaia Z (2006) Stem cells for the treatment of neurological disorders. Nature 441:1094–1096.
4. Cummings BJ, et al. (2005) Human neural stem cells differentiate and promote locomotor recovery in spinal cord-injured mice. Proc Natl Acad Sci USA 102: 14069–14074.
5. Salazar DL, Uchida N, Hamers FP, Cummings BJ, Anderson AJ (2010) Human neural stem cells differentiate and promote locomotor recovery in an early chronic spinal cord injury NOD-scid mouse model. PLoS ONE 5:e12272.
6. Hofstetter CP, et al. (2005) Allodynia limits the usefulness of intraspinal neural stem cell grafts; directed differentiation improves outcome. Nat Neurosci 8:346–353.
7. Ogawa Y, et al. (2002) Transplantation of in vitro-expanded fetal neural progenitor cells results in neurogenesis and functional recovery after spinal cord contusion injury in adult rats. J Neurosci Res 69:925–933.
8. Iwanami A, et al. (2005) Transplantation of human neural stem cells for spinal cord injury in primates. J Neurosci Res 80:182–190.
9. Okada S, et al. (2005) In vivo imaging of engrafted neural stem cells: Its application in evaluating the optimal timing of transplantation for spinal cord injury. FASEB J 19: 1839–1841.
10. Okada Y, Shimazaki T, Sobue G, Okano H (2004) Retinoic-acid-concentration-dependent acquisition of neural cell identity during in vitro differentiation of mouse embryonic stem cells. Dev Biol 275:124–142.
11. Okada Y, et al. (2008) Spatiotemporal recapitulation of central nervous system development by murine embryonic stem cell-derived neural stem/progenitor cells. Stem Cells 26:3086–3098.
12. Kumagai G, et al. (2009) Roles of ES cell-derived gliogenic neural stem/progenitor cells in functional recovery after spinal cord injury. PLoS ONE 4:e7706.
13. Keirstead HS, et al. (2005) Human embryonic stem cell-derived oligodendrocyte progenitor cell transplants remyelinate and restore locomotion after spinal cord injury. J Neurosci 25:4694–4705.
14. Sharp J, Frame J, Siegenthaler M, Nistor G, Keirstead HS (2010) Human embryonic stem cell-derived oligodendrocyte progenitor cell transplants improve recovery after cervical spinal cord injury. Stem Cells 28:152–163.
15. Strauss S (2010) Geron trial resumes, but standards for stem cell trials remain elusive. Nat Biotechnol 28:989–990.
16. Takahashi K, Yamanaka S (2006) Induction of pluripotent stem cells from mouse embryonic and adult fibroblast cultures by defined factors. Cell 126:663–676.
17. Okita K, Ichisaka T, Yamanaka S (2007) Generation of germline-competent induced pluripotent stem cells. Nature 448:313–317.
18. Tsuji O, et al. (2010) Therapeutic potential of appropriately evaluated safe-induced pluripotent stem cells for spinal cord injury. Proc Natl Acad Sci USA 107:12704–12709.
19. Takahashi K, et al. (2007) Induction of pluripotent stem cells from adult human fibroblasts by defined factors. Cell 131:861–872.
20. Bregman BS (1987) Spinal cord transplants permit the growth of serotonergic axons across the site of neonatal spinal cord transection. Brain Res 431:265–279.
21. Saruhashi Y, Young W, Perkins R (1996) The recovery of 5-HT immunoreactivity in lumbosacral spinal cord and locomotor function after thoracic hemisection. Exp Neurol 139:203–213.
22. Kim D, et al. (1999) Direct agonists for serotonin receptors enhance locomotor function in rats that received neural transplants after neonatal spinal transection. J Neurosci 19:6213–6224.
23. Kobayashi NR, et al. (1997) BDNF and NT-4/5 prevent atrophy of rat rubrospinal neurons after cervical axotomy, stimulate GAP-43 and Talpha1-tubulin mRNA expression, and promote axonal regeneration. J Neurosci 17:9583–9595.
24. Krenz NR, Weaver LC (1998) Sprouting of primary afferent fibers after spinal cord transection in the rat. Neuroscience 85:443–458.
25. Krenz NR, Meakin SO, Krassioukov AV, Weaver LC (1999) Neutralizing intraspinal nerve growth factor blocks autonomic dysreflexia caused by spinal cord injury. J Neurosci 19:7405–7414.
26. Li S, Kim JE, Budel S, Hampton TG, Strittmatter SM (2005) Transgenic inhibition of Nogo-66 receptor function allows axonal sprouting and improved locomotion after spinal injury. Mol Cell Neurosci 29:26–39.
27. Springer JE, et al. (2010) The functional and neuroprotective actions of Neu2000, a dual-acting pharmacological agent, in the treatment of acute spinal cord injury. J Neurotrauma 27:139–149.
28. Beattie MS, et al. (1997) Endogenous repair after spinal cord contusion injuries in the rat. Exp Neurol 148:453–463.
29. Kim HM, Hwang DH, Lee JE, Kim SU, Kim BG (2009) Ex vivo VEGF delivery by neural stem cells enhances proliferation of glial progenitors, angiogenesis, and tissue sparing after spinal cord injury. PLoS ONE 4:e4987.
30. Yoshida H, et al. (2002) Platelet-activating factor enhances the expression of vascular endothelial growth factor in normal human astrocytes. Brain Res 944:65–72.
31. Mense SM, et al. (2006) Gene expression profiling reveals the profound upregulation of hypoxia-responsive genes in primary human astrocytes. Physiol Genomics 25: 435–449.
32. Hofstetter CP, et al. (2002) Marrow stromal cells form guiding strands in the injured spinal cord and promote recovery. Proc Natl Acad Sci USA 99:2199–2204.
33. Jones LL, Oudega M, Bunge MB, Tuszynski MH (2001) Neurotrophic factors, cellular bridges and gene therapy for spinal cord injury. J Physiol 533:83–89.
34. Brock JH, et al. (2010) Local and remote growth factor effects after primate spinal cord injury. J Neurosci 30:9728–9737.
35. Jakeman LB, Wei P, Guan Z, Stokes BT (1998) Brain-derived neurotrophic factor stimulates hindlimb stepping and sprouting of cholinergic fibers after spinal cord injury. Exp Neurol 154:170–184.
36. Tuszynski MH, et al. (1996) Nerve growth factor delivery by gene transfer induces differential outgrowth of sensory, motor, and noradrenergic neurites after adult spinal cord injury. Exp Neurol 137:157–173.
37. Tuszynski MH (1997) Gene therapy for nervous system disease. Ann N Y Acad Sci 835: 1–11.
38. Kitamura K, et al. (2007) Hepatocyte growth factor promotes endogenous repair and functional recovery after spinal cord injury. J Neurosci Res 85:2332–2342.
39. Abematsu M, et al. (2010) Neurons derived from transplanted neural stem cells restore disrupted neuronal circuitry in a mouse model of spinal cord injury. J Clin Invest 120:3255–3266.
40. Mitsui T, Shumsky JS, Lepore AC, Murray M, Fischer I (2005) Transplantation of neuronal and glial restricted precursors into contused spinal cord improves bladder and motor functions, decreases thermal hypersensitivity, and modifies intraspinal circuitry. J Neurosci 25:9624–9636.
41. Kim BG, Dai HN, Lynskey JV, McAtee M, Bregman BS (2006) Degradation of chondroitin sulfate proteoglycans potentiates transplant-mediated axonal remodeling and functional recovery after spinal cord injury in adult rats. J Comp Neurol 497: 182–198.
42. White TE, et al. (2010) Neuronal progenitor transplantation and respiratory outcomes following upper cervical spinal cord injury in adult rats. Exp Neurol 225:231–236.
43. Bonner JF, Blesch A, Neuhuber B, Fischer I (2010) Promoting directional axon growth from neural progenitors grafted into the injured spinal cord. J Neurosci Res 88: 1182–1192.
44. Schneider SP, Fyffe RE (1992) Involvement of GABA and glycine in recurrent inhibition of spinal motoneurons. J Neurophysiol 68:397–406.
45. Malcangio M, Bowery NG (1996) GABA and its receptors in the spinal cord. Trends Pharmacol Sci 17:457–462.
46. Kim DS, et al. (2010) Transplantation of gabaergic neurons from ES cells attenuates tactile hypersensitivity following spinal cord injury. Stem Cells 28:2099–2108.
47. Watanabe K, et al. (2004) Comparison between fetal spinal-cord- and forebrain-derived neural stem/progenitor cells as a source of transplantation for spinal cord injury. Dev Neurosci 26:275–287.
48. Ogawa D, et al. (2009) Evaluation of human fetal neural stem/progenitor cells as a source for cell replacement therapy for neurological disorders: Properties and tumorigenicity after long-term in vitro maintenance. J Neurosci Res 87:307–317.
49. Yan J, et al. (2007) Extensive neuronal differentiation of human neural stem cell grafts in adult rat spinal cord. PLoS Med 4:e39.
50. Fusaki N, Ban H, Nishiyama A, Saeki K, Hasegawa M (2009) Efficient induction of transgene-free human pluripotent stem cells using a vector based on Sendai virus, an RNA virus that does not integrate into the host genome. Proc Jpn Acad, Ser B, Phys Biol Sci 85:348–362.
51. Okita K, Nakagawa M, Hyenjong H, Ichisaka T, Yamanaka S (2008) Generation of mouse induced pluripotent stem cells without viral vectors. Science 322:949–953.
52. Zhou H, et al. (2009) Generation of induced pluripotent stem cells using recombinant proteins. Cell Stem Cell 4:381–384.
53. Warren L, et al. (2010) Highly efficient reprogramming to pluripotency and directed differentiation of human cells with synthetic modified mRNA. Cell Stem Cell 7: 618–630.
54. Rhee YH, et al. (2011) Protein-based human iPS cells efficiently generate functional dopamine neurons and can treat a rat model of Parkinson disease. J Clin Invest 121: 2326–2335.
55. Okita K, et al. (2011) A more efficient method to generate integration-free human iPS cells. Nat Methods 8:409–412.
56. Miura K, et al. (2009) Variation in the safety of induced pluripotent stem cell lines. Nat Biotechnol 27:743–745.
57. Scheff SW, Rabchevsky AG, Fugaccia I, Main JA, Lumpp JE, Jr. (2003) Experimental modeling of spinal cord injury: Characterization of a force-defined injury device. J Neurotrauma 20:179–193.